Effect of Design Parameters on the Blast Response of Ultra-High Performance Concrete Columns

Author(s) & Affiliation: Sarah De Carufel[1], Frederic Dagenais[1], Christian Melançon[1] and Hassan Aoude[2]

[1]Master's Student, University of Ottawa

[2]Associate Professor, University of Ottawa

Abstract: This paper summarizes the results of an ongoing research program examining the blast performance of UHPC columns. As part of the study eight columns built with conventional concrete and UHPC were tested under simulated blast loading using a shock-tube. Parameters considered in this study include effect of concrete type, fiber properties, fiber content, transverse reinforcement, longitudinal reinforcement ratio and strength. The results demonstrate that the use of UHPC results in important performance enhancements in columns subjected to blast loads, including reduced displacements, increased blast resistance and improved damage tolerance.

Keywords: UHPC, Columns, Blast, Shock-tube, high-strength steel

1. Introduction

When compared to conventional concrete, ultra-high performance concrete (UHPC) shows higher compressive strength, increased tensile resistance and superior toughness. These enhanced properties make UHPC an ideal material for use in the design of blast resistant structures. In ground-story concrete building columns the use of UHPC can potentially be used to relax required detailing, while providing the strength necessary to prevent progressive collapse. This paper summarizes the results from an ongoing research program at the University of Ottawa examining the performance the potential of using UHPC to improve the blast performance of reinforced concrete structural components. As part of the current study, eight columns were tested under varying pressure-impulse combinations using a high-capacity shock-tube. Parameters considered include effect of concrete type, fiber properties, fiber content, transverse reinforcement spacing, longitudinal reinforcement ratio and longitudinal reinforcement strength. The results are compared in terms of the effect of the parameters on the control of column displacements, overall blast resistance and failure mode.

2. Background

2.1 Previous Research on Blast Performance of UHPC

Experimental studies on the blast performance of UHPC have primarily focused on the behavior of one-way panels. Ngo et al. (2007) tested seven UHPC panels under live explosives at standoff distances of 30-50 m (98 - 164 ft). In contrast to companion panels constructed with conventional concrete, the UHPC panels showed high ductility, limited permanent deformations, and an ability to absorb substantial energy without fragmentation. Wu et al. (2009) tested a further series of UHPC panels under 1-20 kg of equivalent TNT at small standoffs of 1-3 m (3.3 - 9.8 ft). The panels showed an ability to sustain larger blast loads when compared to companion panels made of conventional concrete. In a further study, Barnett et al. (2010) tested four simply-supported

UHPC panels under larger charge weights of 100 kg of equivalent TNT at standoff distances of 7m and 9 m (23 and 29 ft) and found the UHPC panels capable recovering large maximum displacements with small residual displacements and no major fragmentation at failure. Ellis et al. (2014) tested four unreinforced one-way UHPC panels having dimensions using a blast simulator. The study demonstrated that factors that increase energy dissipation, such as fiber geometry, fiber packing and fiber volume fraction, are critical to enhancing the blast performance of unreinforced UHPC panels. The potential of using UHPC to improve the blast resistance of columns has been studied numerically by Astarioglu and Krauthammer (2014). The results of this numerical investigation showed the UHPC columns to have reduced displacements under equivalent blasts when compared to columns made of ordinary concrete, with an ability to sustain higher impulse loads before failure. In summary, research confirms improved performance of UHPC under blast loading, however there is need for further data, particularly in the case of columns.

3. Methods

3.1 Description of Specimens

A total of eight column specimens were tested in this study in order to investigate the effect of UHPC on the response of columns subjected to blast loading. Table 1 and Figure 1 summarize the properties and design details of the column specimens. The series included one control column constructed with plain self-consolidating concrete (SCC) and seven columns constructed with compact reinforced composite (CRC), a proprietary UHPC (Aarup, 1998). All columns had cross-sectional dimensions of 152 mm x 152 mm (6 in x 6 in). The clear cover was 5 mm (0.2 in) and the transverse reinforcement consisted of 6.3 mm (0.25 in) diameter ties having a centre-to-centre spacing of 75 mm (3.0 in) and 38 mm (1.5 in), representing "non-seismic" and "seismic" detailing, respectively. The longitudinal reinforcement in the first six columns consisted of either 4-10M or 4-15M Canadian size normal-strength bars (Area = 100 mm^2 [0.16 in^2] and 200 mm^2 [0.32 in^2]), resulting in reinforcement ratios of 1.73% and 3.46%, respectively. One column was constructed with 6-#3 American size high-strength (HS) bars (Area = 71 mm^2 [0.11 in^2]), corresponding to a reinforcement ratio 1.84%. As shown in Table 1, the specimen nomenclature reflects the variables in the study, including: concrete type (SCC or CRC), fiber content (0 to 4%), fiber type (A, B or C), tie spacing (75 or 38 mm) and longitudinal reinforcement ratio/strength (15M or 6#3HS to indicate the use of 15M and #3 HS steel bars, respectively).

Table 1: Column design details

Column ID	Concrete type	Fiber type & content	Concrete compressive strength f'c MPa (ksi)	Tie spacing mm (in)	Longitudinal reinforcement
SCC-0%-75	SCC	-	52 (7.5)	75 (3.0)	4 - 10M
CRC-2%A-75	CRC	2% A	145 (21.0)	75 (3.0)	
CRC-4%A-75		4% A	153 (22.2)	75 (3.0)	
CRC-2%A-38		2% A	149(21.6)	38 (1.5)	
CRC-2%B-75		2% B	138 (20.0)	75 (3.0)	
CRC-2%C-75		2% C	145 (21.0)	75 (3.0)	
CRC-2%B-75-15M		2% B	138 (20.0)	75 (3.0)	4-15M
CRC-2%B-75-6#3-HS		2% B	150(21.8)	75 (3.0)	6#3 (HS)

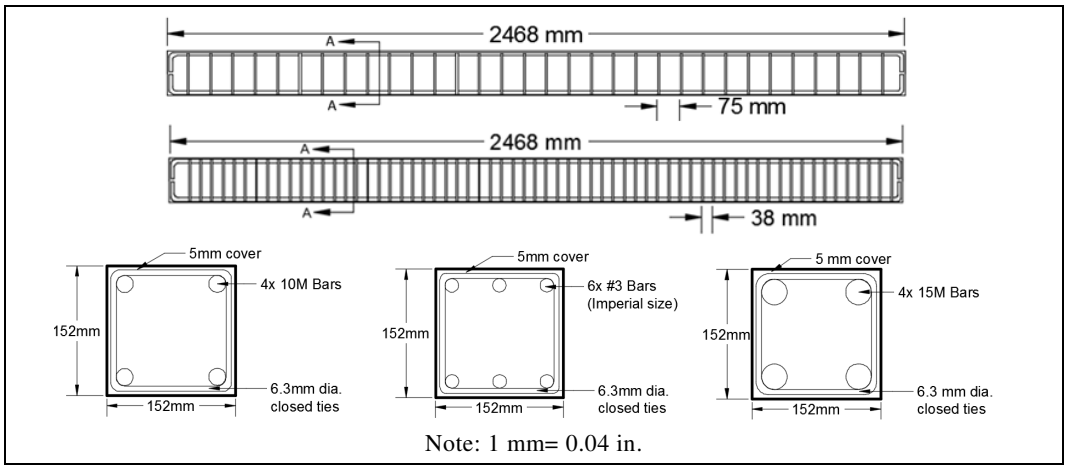

Figure 1: Column design details

3.2 Material Properties

The control column was built using self-consolidating concrete (SCC) having a specified strength of 50 MPa (7.3 ksi) (Burrell et al. 2015). The UHPC specimens were constructed with compact reinforced composite (CRC) with a specified strength of 140 MPa. The mix was reinforced with straight smooth fibers at volumetric ratios of 2-4%. Three different fibers were considered in this study; fiber types A, B and C had aspect ratios (length/diameter) of 32(13 mm /0.4 mm), 62(13 mm/0.21 mm) and 43(13mm/ 0.3 mm), with tensile strengths of 1350, 2750 and 3150 MPa (196, 400 and 457 ksi), respectively. Figure 2a shows typical stress-strain curves for the plain SCC and CRC with 2% B fibers, obtained by testing 100 mm x 200 mm [4 in x 6 in] cylinders. Three types of longitudinal steel bars were used in this study. The yield strengths of the 10M and 15M steel bars were 486 MPa (70 ksi) and 460 MPa (67 ksi), respectively. The #3 size high-strength (HS) bars were made of a corrosion-resistant low-carbon chromium-steel alloy, with a strength at yielding/at failure of approximately 950/1200 MPa (138/174 ksi) (MMFX, 2013). Typical stress-strain curves are shown in Figure 2b for both the ordinary and high-strength steel bars. The steel used in the column ties had a yield strength of 604 MPa (88 ksi).

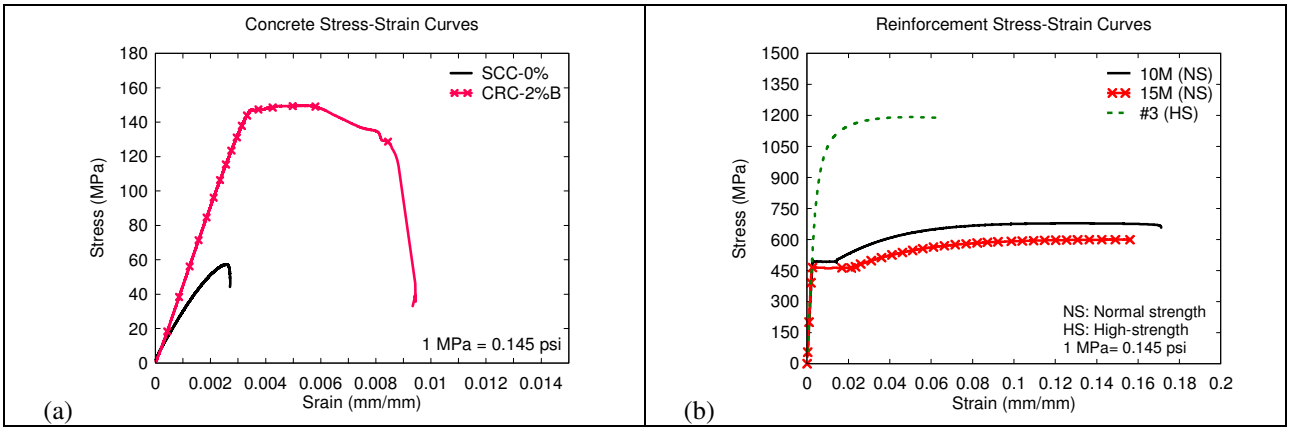

Figure 2: Typical stress-strain curves for (a) concrete in compression and (b) steel in tension

3.3 Test Procedure

All specimens were tested under simulated blast loads using the University of Ottawa shock-tube. The shockwaves are generated using compressed air which is rapidly released into and expansion chamber and travels until it reaches the specimen. As shown in Figure 3a, the shock-tube is composed of a variable length driver section which generates the shockwave, a spool section which controls the release of the shockwave, and an expansion section which expands to a square test frame (Lloyd et al. 2011). Figure 3b shows the setup for the column tests. A load-transfer device (LTD) made of sheet-metal and a series of steel beams was used to transfer the shockwave as a distributed load onto the column specimens over a clear span of 1980 mm (78 in.) between the supports. All columns had partially-fixed end-restraints and were tested under combined transverse shockwave load and an axial load corresponding to 30% of the nominal capacity of the control SCC specimen (~ 300 KN [67 kips]). Maximum and residual displacements were measured using linear variable displacement transducers (LVDT) placed at mid-height. In addition, a high speed video camera was used to record the testing at a frame rate of 500 frames per second.

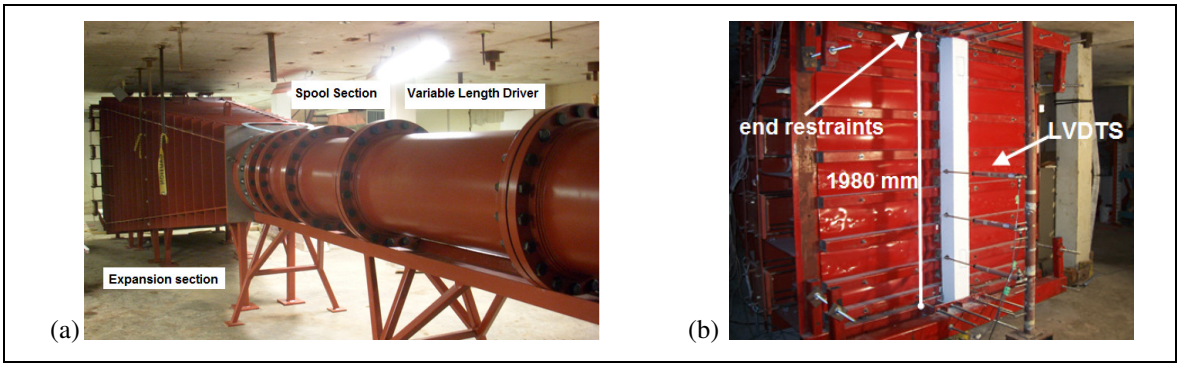

Figure 3: (a) University of Ottawa shock-tube and (b) column test setup.

Each specimen was subjected to gradually increasing blast loads until failure; Blast 1 aimed at keeping the columns within the elastic range, while Blast 2 and Blasts 3/4/5 aimed at testing the columns at yield and ultimate conditions. The average shockwave properties such as reflected pressure, positive time duration, reflected impulse and typical pressure time histories for Blasts 1-2-3-4-5 are presented in Figure 4..

Blast	Reflected Pressure kPa (Psi)	Positive Phase Duration msec	Reflected Impulse kPa*ms (Psi-mse)
Blast 1	15(2)	21.4	125 (18)
Blast 2	45 (7)	23.0	400 (58)
Blast 3	80 (12)	26.2	750 (108)
Blast 4	97 (14)	25.1	900 (131)
Blast 5	85 (12)	33.0	1355 (197)

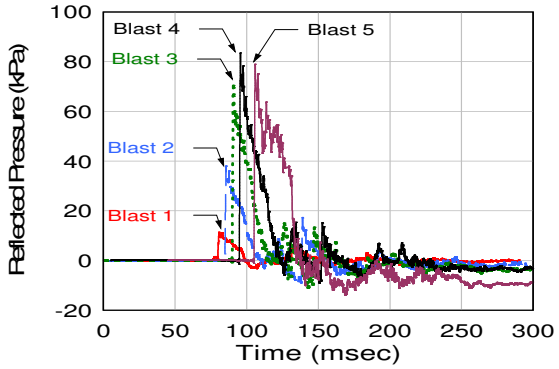

Figure 4: Average blast properties (Blast 1 to 5)

4. Results

All columns had similar response under Blast 1 and 2 loading. To investigate the effect of the test parameters, Table 2 and Figure 5 compare the maximum and residual midspan displacements of all columns at Blasts 3-4-5, along with identification of failure mode. As identifies below some columns required to be submitted to an additional Blast 4, identified as Blast4(2), to cause failure of the specimen, Discussions on the effect of the various test parameters are provided in the following sections.

Table 2: Test results at Blast 3 and 4

	Blast 3		Blast 4		Blast 5		Failure
Column ID	d_{max} mm (in.)	d_{res} mm (in.)	d_{max} mm (in.)	d_{res} mm (in.)	d_{max} mm (in)	d_{res} mm (in.)	
SCC-0%-75	129 (5.1)	109 (4.3)	-	-	-	-	Blast 3: Extensive concrete crushing Long. compression reinf. buckling
CRC-2%A-75	68 (2.7)	22 (0.9)	310 (12.2)	288 (11.3)	-	-	Blast 4: Long. tension reinf. rupture Concrete fiber pull-out
CRC-4%A-75	57 (2.2)	14 (0.6)	94 (3.7)	26 (1.0)	-	-	Blast 4(2) :Long. Tension reinf. rupture Concrete fiber pull-out
CRC-2%A-38	47 (1.9)	8 (0.3)	71 (2.8)	13 (0.5)	270 (10.6)	242 (9.5)	Blast 5: Long. tension reinf. rupture Concrete fiber pull-out
CRC-2%B-75	60 (2.4)	24 (0.9)	No data		-	-	Blast 4: Long. tension reinf. rupture Concrete fiber pull-out
CRC-2%C-75	51 (2.0)	13 (0.5)	No data		-	-	Blast 4: Long. tension reinf. rupture Concrete fiber pull-out
CRC-2%B-75-15M	52 (2.1)	17 (0.7)	88 (3.5)	42 (1.7)	-	-	Blast 4(2) : Wide crack opening No rupture of reinforcement
CRC -2%B-75-6#3-HS	54 (2.1)	17 (0.7)	145 (5.7)	58 (2.3)	-	-	Blast 4(2): 2 out of 3 long. tension reinf. rupture, Concrete fiber pull-out

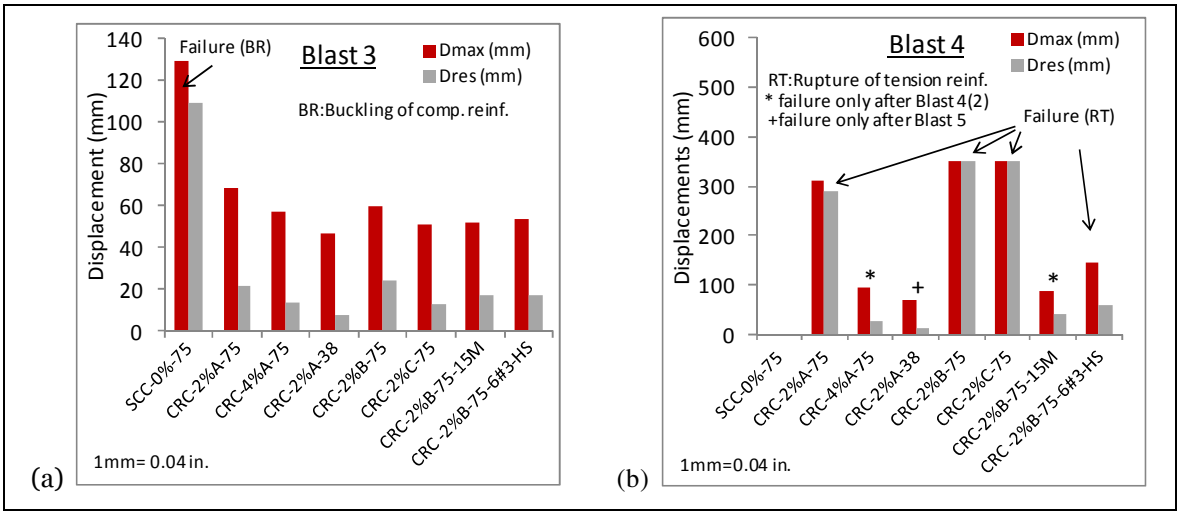

Figure 5: Comparison of maximal and residual displacements at (a) Blast 3 and (b) Blast 4

4.1 Effect of Concrete Type

The effect of concrete type can be investigated by comparing the response of columns CRC-2%A-75 and SCC-0%-75, which had identical reinforcement but were constructed with CRC and SCC, respectively. Examination of the displacement data in Table 2 and Figure 5 for specimens CRC-2%A-75 and SCC-0%-75 shows that the use of UHPC led to significant improvements in column blast performance. Under Blast 3, maximum and residual displacements were reduced by 46% and 80% in column CRC-2%A-75 when compared to the control column. The use of UHPC also had an important effect on overall blast resistance and failure mode. Failure of specimen SCC-0%-75 occurred after Blast 3 and resulted in extensive concrete damage and buckling of compression steel reinforcement (see Figure 6a). In contrast, the CRC specimen showed relatively minor damage and prevented rebar buckling at this blast, with additional loading corresponding to Blast 4 required to cause failure, which occurred due to rupture of tension steel (see Figure 6b). The use of UHPC also had an important effect on the reduction of secondary blast fragments. Figure 6e & Figure 6f compare high-speed video stills of the columns at failure; it is clear that while the SCC specimen shows significant fragmentation, the CRC column shows an ability to eliminate secondary blast fragments, event at failure.

4.2 Effect of Fiber Content

The effect of fiber content can be investigated by comparing the response of columns CRC-2%A-75 and CRC-4%A-75, which were reinforced with 2% and 4% of fiber type A, respectively. Comparison of the displacements in Table 2 and Figure 5 shows improved displacement control with increase in fiber content from 2% to 4%. At Blast 3 Column CRC-4%A-75 shows reductions of 16% and 36% for maximal and residual displacements, respectively when compared to column CRC-2%A-75. The increase in fiber content also provided higher ultimate blast resistance; column CRC-2%A-75 failed due to rupture of tension steel at Blast 4, while the increased fiber content in column CRC-4%A-75 was sufficient to prevent failure under this impulse, with failure delayed to Blast 5.

4.3 Effect of Fiber Type

The effect of fiber type can be examined by comparing the response of columns CRC-2%A-75, CRC-2%B-75 and CRC-2%C-75, which had identical properties but were reinforced with 2% of fiber types A, B and C. Comparison of the displacements in Table 2 and Figure 5 shows improvement in blast response for fiber types B and C which had enhanced properties when compared to fiber type A. For example, under Blast 3, column CRC-2%C-75 shows reductions in maximum and residual displacements of 25% and 40% when compared to column CRC-2%A-75. In addition to an increase in fiber aspect-ratio (43 vs. 32), fiber C had a 133% increase in tensile strength [3150 vs. 1350 MPa (457 vs. 196 ksi)] when compared to fiber A.

4.4 Effect of Seismic Detailing

The effect of seismic detailing can be studied by comparing the response of columns CRC-2%A-75 and CRC-2%A-38 which had transverse reinforcement spacing of s = 75 & 38 mm (3 & 1.5 in.), corresponding to non-seismic and seismic detailing, respectively. As shown in Table 2 and Figure 5, the use of seismic detailing in CRC-2%A-38 resulted in reductions in maximum and residual displacements by factors of 30% and 63% at Blast 3 when compared to CRC-2%A-75.

The use of closely spaced ties also had an effect on overall blast capacity; failure of specimen CRC-2%A-75 occurred at Blast 4, while a second application of Blast 4 was required to cause failure in column CRC-2%A-38.

4.5 Effect of Reinforcement Ratio and High Strength Reinforcement

As noted in the previous sections, failure of all CRC columns containing 10M longitudinal reinforcement occurred due to rupture of the tension steel bars at extreme blast pressures. The rupture of the tension reinforcement can be linked to the high compressive strength of CRC which leads to the development of high tensile strains in the tension reinforcement in columns subjected to flexural blast loading. The provision of increased reinforcement ratio or high-strength reinforcement are potential solutions for this problem. The effect of longitudinal ratio and strength can be investigated by comparing the response of columns CRC-2%B-75, CRC-2%B-75-15M and CRC-2%B-6#3-HS. Under Blast 3, maximum and residual displacements were reduced by factors of approximately 10% and 30% for the columns with 15M and #3-HS reinforcement, when compared to column CRC-2%B-75 which contained ordinary 10M bars (see Table 2 and Figure 5). At Blast 4 the use of 15M bars in CRC-2%B-75-15M prevented rupture of tension steel, and allowed the column to sustain a second application of Blast 4 pressures before failure (see Figure 6d). For the specimen containing high-strength reinforcement (CRC-2%B-6#3-HS), two out of the three tension steel reinforcing bars did not rupture at Blast 4, resulting in a more controlled failure when compared to column CRC-2%B-75 (see Figure 6c).

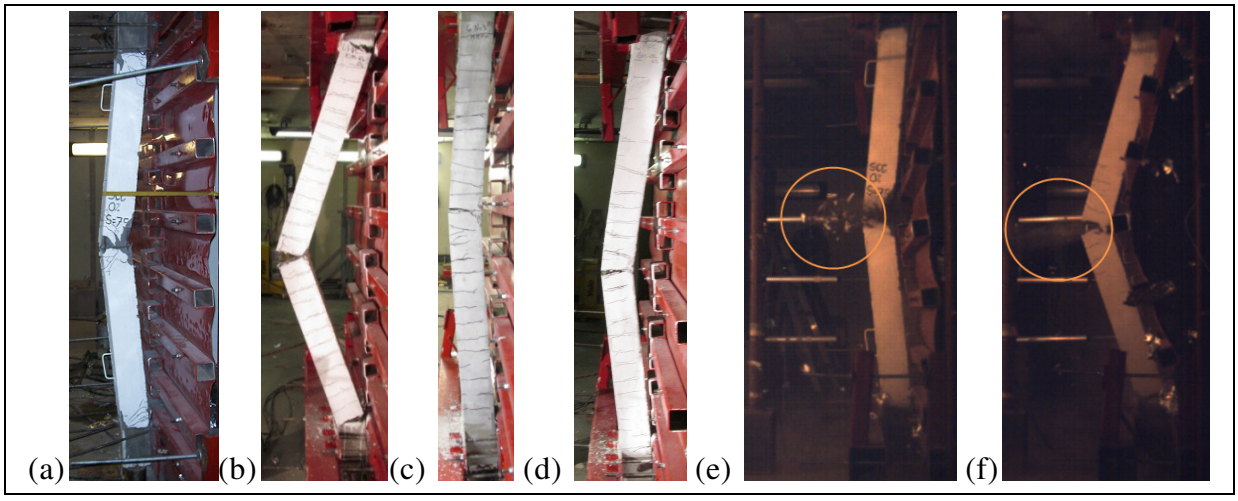

Figure 6: (a) Damage in column SCC-0%-75 at failure [Blast 3], (b) damage in column CRC-2%B-75 at failure [Blast 4], (c) damage in column CRC-2%B-75-6#3-HS at failure [Blast 4], (d) damage in column CRC-2%B-75-15M at failure [Blast 4(2)], (e) video still of column SCC-0%-75 at Blast 3 and (f) video still of column CRC-2%A-75 at Blast 4.

5. Conclusions

The paper presented the results from eight columns tested under simulated blast loading using a shock-tube. The following conclusions are drawn from this study:

- The use of UHPC improves blast performance, allowing for a better control of displacements, and an ability to sustain larger blast pressures before failure;
- The use of UHPC significantly improves damage tolerance of columns under blast loading, with an ability to eliminate secondary blast fragments, even at failure;

- In this study, increasing fiber content from 2% to 4% and the use of seismic detailing improved the blast performance of the UHPC columns, and resulted in reduced displacements and an ability to sustain larger blast loads before failure;
- The use of fibers with optimized properties (increased aspect-ratio and tensile strength) led to improvements in the blast performance of the UHPC columns, with reductions in displacements at equivalent blasts loads;
- Increasing the reinforcement ratio was shown to delay rupture of tension steel reinforcement in UHPC columns subjected to extreme blast loads. Similar results were obtained when combining UHPC with high-strength steel reinforcement.

6. References

Burrell R.P., Aoude, H., and Saatcioglu M., "Response of SFRC Columns under Blast Loads." *ASCE Journal of Structural Engineering*, Vol. 80, No. 9, 2015, pp. 1-218.

Astarlioglu, S., Krauthammer, T., "Response of normal-strength and ultra-high-performance fiber-reinforced concrete columns to idealized blast loads," *Engineering Structures;* Vol. 61, March, 2014, pp. 1-12.

Bache, H.H., "Compact reinforced composite: basic principles," Aalborg, Portland, CBL Report No. 41, 1987.

Barnett, S., Millard, S., Tyas, A., Schleyer G., "Blast tests of fibre-reinforced concrete panel," *Proceedings of the ICE - Construction Materials*, Vol. 163, No.3, August, 2010, pp. 127-129.

Ellis, B.D., DiPaolo, B.P., McDowell, D.L., Zhou, M., "Experimental investigation and multiscale modeling of ultra-high-performance concrete panels subject to blast loading," *International Journal of Impact Engineering*, Vol. 69, July, 2014, pp. 95-103.

Lloyd, A., Jacques, E., Saatcioglu, M., Palermo, D., Nistor, I., Tikka, T., "Capabilities and effectiveness of using a shock tube to simulate blast loading on structures and structural components," *ACI Special Publication 281: Behavior of concrete structures to blast and impact loads*, Vol. 281, No. 3, 2011, pp. 1-20.

Ngo, T., Mendis, P., Krauthammer, T., "Behavior of ultrahigh-strength prestressed concrete panels subjected to blast loading," *ASCE Journal of Structural Engineering*, Vol. 133, No.11, November, 2007, pp. 1582-1590.

Wu, C., Oehlers, D. J., Rebentrost, M., Leach, J., Whittaker, A. S., "Blast testing of ultra-high performance fibre concrete slabs and FRP retrofitted RC slabs," *Engineering Structures*, Vol.31, No. 9, September, 2009, pp. 2060-2069.

7. Acknowledgements

The authors would like to thank CRC Technology (Hi-Con A/S) and MMFX Technologies Corporation for providing the materials used in this study.